SCIENCE CHINA
Physics, Mechanics & Astronomy

• Article •

March 2024 Vol. 67 No. 3: 237411
https://doi.org/10.1007/s11433-023-2287-8

High-order time-reversal symmetry breaking normal state

Meng Zeng[1], Lun-Hui Hu[2], Hong-Ye Hu[1], Yi-Zhuang You[1], and Congjun Wu[3,4,5,6*]

[1]*Department of Physics, University of California, San Diego, California 92093, USA;*
[2]*Department of Physics, Zhejiang University, Hangzhou 310058, China;*
[3]*New Cornerstone Science Laboratory, Department of Physics, School of Science, Westlake University, Hangzhou 310024, China;*
[4]*Institute for Theoretical Sciences, Westlake University, Hangzhou 310024, China;*
[5]*Key Laboratory for Quantum Materials of Zhejiang Province, School of Science, Westlake University, Hangzhou 310024, China;*
[6]*Institute of Natural Sciences, Westlake Institute for Advanced Study, Hangzhou 310024, China*

Received October 13, 2023; accepted November 22, 2023; published online February 2, 2024

Spontaneous time-reversal symmetry breaking plays an important role in studying strongly correlated unconventional superconductors. When two superconducting gap functions with different symmetries compete, the relative phase channel ($\theta_- \equiv \theta_1 - \theta_2$) exhibits an Ising-type Z_2 symmetry due to the second order Josephson coupling, where $\theta_{1,2}$ are the phases of two gap functions. In contrast, the $U(1)$ symmetry in the channel of $\theta_+ \equiv \frac{\theta_1+\theta_2}{2}$ is intact. The phase locking, i.e., ordering of θ_-, can take place in the phase fluctuation regime before the onset of superconductivity, i.e., when θ_+ is disordered. If θ_- is pinned at $\pm\frac{\pi}{2}$, then time-reversal symmetry is broken in the normal state, otherwise, if $\theta_- = 0$, or, π, rotational symmetry is broken, leading to a nematic normal state. In both cases, the order parameters possess a 4-fermion structure beyond the scope of mean-field theory, which can be viewed as a high order symmetry breaking. We employ an effective two-component XY-model assisted by a renormalization group analysis to address this problem. As a natural by-product, we also find the other interesting intermediate phase corresponds to ordering of θ_+ but with θ_- disordered. This is the quartetting, or, charge-4e, superconductivity, which occurs above the low temperature Z_2-breaking charge-2e superconducting phase. Our results provide useful guidance for studying novel symmetry breaking phases in strongly correlated superconductors.

superconductivity, strong correlation, time-reversal breaking, charge-4e

PACS number(s): 71.27.+a, 74.20.-z, 74.20.De, 74.25.Dw

Citation: M. Zeng, L.-H. Hu, H.-Y. Hu, Y.-Z. You, and C. Wu, High-order time-reversal symmetry breaking normal state, Sci. China-Phys. Mech. Astron. **67**, 237411 (2024), https://doi.org/10.1007/s11433-023-2287-8

1 Introduction

Unconventional superconductors (for instance, high-T_c cuprates [1], heavy-fermion systems [2], and iron-based superconductors [3]) have aroused a great deal of attentions for novel symmetries in addition to the $U(1)$ symmetry breaking. Time-reversal symmetry (TRS) as well as parity and charge conjugation are fundamental discrete symmetries, hence, spontaneous TRS-breaking superconductivity is of particular importance [4-14]. Various TRS-breaking pairing structures are theoretically proposed, including $d \pm \mathrm{i}d$ [15, 16], $p \pm \mathrm{i}p$ [11,17], $s\pm\mathrm{i}d$ [4,18], $p\pm\mathrm{i}s$ [19], and $s+\mathrm{i}s$ [14,20], and experimental evidence has been reported in various systems, such as Re_6Zr [21, 22], UPt_3 [23, 24], $PrOs_4Sb_{12}$ [25], URu_2Si_2 [26, 27], SrPtAs [28], $LaNiC_2$ [29], $LaNiGa_2$ [30, 31], Bi/Ni bilayers [32], and CaPtAs [33] (For details refer to a recent review [34]). They are often probed by the zero-field μ-spin relaxation, or, rotation [35-37], and the polar Kerr effect

*Corresponding author (email: wucongjun@westlake.edu.cn)

© Science China Press 2024

[38, 39]. TRS breaking signatures have also been reported in iron-based superconductors [40, 41].

If TRS breaking arises from a complex pairing structure, it is often presumed that it develops after the onset of superconductivity. However, these two transitions are of different nature: Superconductivity is of the $U(1)$ symmetry breaking and TRS is of Z_2, hence, they could take place at different temperatures. It is interesting to further check whether TRS breaking can occur before the superconducting transition as the temperature is lowered. In fact, phase fluctuations are prominent in strongly correlated superconductors above but close to T_c, such as high T_c cuprates [42] and iron-based superconductors [43].

In a two-gap superconductor, the TRS breaking can be solely determined by the relative phase between two gap functions. The phases of two channels may fluctuate in a coordinated way such that the relative phase is locked, leading to TRS breaking, while the total phase θ_+ is disordered, hence, the system remains normal. In the context of 2D bosons in the p-band, a TRS breaking Mott-insulating ground state was studied via the Ginzburg-Landau free energy analysis and the quantum Monte Carlo simulations [44, 45]. The TRS breaking normal state has been studied in the context of three-gap superconductors as a consequence from frustrations [46].

In this article, we show that there exists an Ising symmetry breaking normal phase in a generic 2D two-gap superconductors when the gap functions belong to different symmetries and are near degeneracy. The key ingredient here, as mentioned above, is the superconduct phase fluctuations. Hence, it is a phase-fluctuation induced TRS-breaking, or, a nematic normal state. By the symmetry principle, the two gap functions couple via a second order Josephson term. Therefore, we dub the resultant symmetry-breaking normal state as the "high-order" symmetry-breaking state. In the phase fluctuation regime, the low energy physics is described by a coupled two-component XY-model, which is mapped to a coupled sine-Gordon model and analyzed by the renormalization group (RG) method. Unlike the small difference in the superconducting transition temperature and the TRS-breaking temperature obtained in ref. [46] from the frustration effects in the three-band model, the phase-locking, or, the Z_2 symmetry breaking temperature can be considerably larger than the superconducting T_c. Another competing order, the quartetting [47], or, charge-4e phase [48], can also appear above T_c, which corresponds to ordered total phase θ_+ but with the relative phase θ_- disordered, i.e., the $U(1)$ symmetry in the θ_+ channel is broken whereas the Z_2 symmetry in the θ_- channel is preserved. All these phases exhibit the 4-fermion-type order parameters, and thus are difficult to analyze in mean-field theories. Quite remarkably, the Z_2-breaking TRS-breaking normal state has recently been experimentally observed in hole-doped $Ba_{1-x}K_xFe_2As_2$ [49, 50], where the TRS-breaking transition is identified with the onset of specific-heat anomaly and spontaneous Nernst signal is also detected in the TRS-breaking normal state. The Z_2-breaking nematic normal state has been observed in Sr_2RuO_4 [51] using optical anisotropy measurement. Even though the normal state nematicity most likely has a different origin from our theory because it can happen at much higher temperature scale, the same experimental techniques can be used to detect nematicity in the phase fluctuation regime proposed in our work. The competing charge-4e state has also been observed recently in kagome superconductor CsV_3Sb_5 [52], where the quantization of magnetic flux in units of $hc/4e$ is observed.

The paper is structured as the following: In sect. 2 we introduce the Ginzberg-Landau theory for superconductors with two gap functions of different symmetries. They couple due to the second order Josephson effect. In sect. 3, we focus on the phase degree of freedom by mapping the theory to a coupled XY-model, which can be further mapped to a coupled sine-Gordon model, setting the stage for the RG study. In sect. 4, we perform detailed RG analysis of the sine-Gordon model by considering the effects of various symmetry-allowed couplings between different channels, which lead to the emergence of different phase diagram topologies. In sect. 5, we briefly discuss the application of our theory to Fe-based superconductors. Then we conclude in sect. 6.

2 Ginzberg-Landau theory with two gap functions

We start with the Ginzberg-Landau (GL) free-energy of superconductivity with two gap functions. Each one by itself is time-reversal invariant. These two gap functions belong to two different representations of the symmetry group, say, the s-wave and d-wave symmetries of a tetragonal system, or, different components of a two-dimensional representation, say, the p_x and p_y-wave symmetries. They cannot couple at the quadratic level since no invariants can mix them at this level. Bearing this in mind, the GL free-energy is constructed as $\mathcal{F} = \mathcal{F}_1 + \mathcal{F}_2$ with

$$\begin{aligned}\mathcal{F}_1 =& \gamma_1|\vec{\nabla}\Delta_1|^2 + \gamma_2|\vec{\nabla}\Delta_2|^2 + \alpha_1(T)|\Delta_1|^2 + \alpha_2(T)|\Delta_2|^2 \\ &+ \beta_1|\Delta_1|^4 + \beta_2|\Delta_2|^4 + \kappa|\Delta_1|^2|\Delta_2|^2, \end{aligned} \tag{1}$$

$$\mathcal{F}_2 = \lambda\left(\Delta_1^2\Delta_2^{*2} + \Delta_1^{*2}\Delta_2^2\right), \tag{2}$$

where $\alpha_{1,2}(T)$ are functions of temperatures, and their zeros determine their superconducting transition temperatures

when the two gap functions decouple. $\gamma_{1,2}$, $\beta_{1,2}$ are all positive and $\kappa^2 < 4\beta_1\beta_2$ to maintain the thermodynamic stability. If the gap functions form a two-dimensional representation of the symmetry group, then $\alpha_1 = \alpha_2$, $\beta_1 = \beta_2$, and $\gamma_1 = \gamma_2$, otherwise, they are generally independent. Nevertheless, we consider the case that they are nearly degenerate, i.e., $\alpha_1 \approx \alpha_2$, when they belong to two different representations, such that they can coexist.

The $\mathcal{F}_1$-term only depends on the magnitude of $\Delta_{1,2}$, hence, is phase insensitive. We assume that the two gap functions can form a quartic invariant as the $\mathcal{F}_2$-term, as in the cases of s and d-waves, and p_x and p_y-wave symmetries. The $\mathcal{F}_2$-term does depend on the relative phase between $\Delta_{1,2}$, which can be viewed as a 2nd order Josephson coupling. To minimize the free energy, the relative phase between two gap functions $\theta_- = \theta_1 - \theta_2 = \pm\frac{\pi}{2}$ at $\lambda > 0$, i.e., they form $\Delta_1 \pm \mathrm{i}\Delta_2$, breaking TRS spontaneously. On the other hand, when $\lambda < 0$, $\theta_- = 0$, or, π. They form the nematic superconductivity $\Delta_1 \pm \Delta_2$, breaking the rotational symmetry. The magnitude of the mixed gap function remains isotropic in momentum space in the former case, while that in the latter case is anisotropic. The value of λ depends on the energetic details of a concrete system. At the mean-field level, the free energy is a convex functional of the gap function distribution in the absence of spin-orbit coupling [5, 19, 53]. This favors a relatively uniform distribution of gap function in momentum space, corresponding to the complex mixing $\Delta_1 \pm \mathrm{i}\Delta_2$, i.e., $\lambda > 0$. Nevertheless, the possibility of $\lambda < 0$ cannot be ruled out, which could take place in the presence of spin-orbit coupling [11], or as a result beyond the mean-field BCS theory. This leads to the gap function $\Delta_1 \pm \Delta_2$, which breaks the rotational symmetry leading to nematic superconductivity.

3 New phases due to the phase fluctuations

The above GL analysis only works in the superconducting phases in which both $\Delta_{1,2}$ develop non-zero expectation values. However, it does not apply to the phase fluctuation regime above T_c. Let us parameterize the gap functions as $\Delta_{1,2} = |\Delta_{1,2}|\mathrm{e}^{\mathrm{i}\theta_{1,2}}$. In the phase fluctuation regime, the order magnitudes $|\Delta_{1,2}|$ are already significant, and their fluctuations can be neglected. On the contrary, the soft phase fluctuations dominate the low energy physics, and the system remains in the normal state before the onset of the long-range phase coherence.

New states can arise in the phase fluctuation regime in which neither of $\Delta_{1,2}$ is ordered. A possibility is that the system remains in the normal state but θ_- is pinned: If $\theta_- = \pm\frac{\pi}{2}$, then $\mathrm{Im}\Delta_1^*\Delta_2$ is ordered, which breaks TRS; if $\theta_- = 0, \pi$, then $\mathrm{Re}\Delta_1^*\Delta_2$ is ordered, which breaks rotation symmetry. Similar physics occurs in the p-orbital band Bose-Hubbard model, where the boson operators in the $p_{x,y}$-bands play the role of $\Delta_{1,2}$, respectively. The transitions of superfluidity and TRS breaking divide the phase diagram into four phases of superfluidity states with and without TRS breaking, and the Mott insulating state with and without TRS breaking, where TRS here corresponds to the development of the onsite orbital angular momentum by occupying the complex orbitals $p_x \pm \mathrm{i}p_y$ [54, 55]. The TRS-breaking normal states were also studied in the context of competing orders in superconductors [56,57]. Another possibility is that the total phase $\theta_+ = \theta_1+\theta_2$ is pinned, i.e., $\Delta_1\Delta_2$ is ordered. This corresponds to the quartetting instability, i.e., a four-fermion clustering instability analogous to the α-particle in nuclear physics. The competition between the pairing and quartetting instabilities in one dimension has been investigated by one of the authors [47]. Later it was also studied in the context of high-T_c cuprates as the charge-4e superconductivity [48].

However, all the above states involve order parameters consisting of 4-fermion operators. Hence, they are beyond the ordinary mean-field theory based on fermion bilinear order parameters. To address these novel states, we map the above GL free-energy to the XY-model on a bilayer lattice, and perform the renormalization group (RG) analysis to study the possible phases. Since there should be no true long-range order of the $U(1)$ symmetry at finite temperatures, we mean the quasi-long-ranged ordering of the Kosterlitz-Thouless (KT) transition. The model is expressed as:

$$H = -J_1 \sum_{\langle i,j\rangle} \cos(\theta_{1i} - \theta_{1j}) - J_2 \sum_{\langle i,j\rangle} \cos(\theta_{2i} - \theta_{2j}) + \lambda' \sum_i \cos 2(\theta_{1i} - \theta_{2i}), \tag{3}$$

where $\theta_{1,2}$ are compact $U(1)$ phases with the modulus 2π. $J_{1,2}$ are the intra-layer couplings estimated as $J_{1,2} \approx \gamma_{1,2}|\Delta_{1,2}|^2$, and λ' is the inter-layer coupling estimated as $\lambda' \approx 2\lambda|\Delta_1|^2|\Delta_2|^2$.

Following the dual representation of the 2D classic XY-model as detailed in the Appendix A1, the above model eq. (3) can be mapped to the following multi-component sine-Gordon model, which is often employed for studying coupled Luttinger liquids [58, 59]. Its Euclidean Lagrangian in the continuum is defined as $L = \int \mathrm{d}^2x\mathcal{L}(x)$ [60], where

$$\mathcal{L}(x) = \frac{1}{2K_1}\left(\partial_\mu\phi_1\right)^2 + \frac{1}{2K_2}(\partial_\mu\phi_2)^2 + g_{\theta_-}\cos 2\left(\theta_1 - \theta_2\right) - g_{\phi_1}\cos 2\pi\phi_1 - g_{\phi_2}\cos 2\pi\phi_2, \tag{4}$$

where $\phi_{1,2}$ are the dual fields to the superconducting phase fields of $\theta_{1,2}$ with commutation relations $[\theta_{1,2}(t,x), \partial_y\phi_{1,2}(t,y)] = 2\pi\mathrm{i}\delta(x-y)$, and the Luttinger parameters $K_{1,2} = J_{1,2}/T$ (Please note that $K_{1,2}$ appear in the

denominators in eq. (4) since we are using the dual representation). The compact radius of $\theta_{1,2}$ is 2π, and that of the vortex fields $\phi_{1,2}$ is 1. g_{θ_-} is proportional to λ' in eq. (3); g_{ϕ_1,ϕ_2} are proportional to the vortex fugacities of the phase fields $\theta_{1,2}$, respectively. For simplicity, all of these g-eology coupling constants have absorbed the short-distance cutoff of the lattice.

4 Renormalization group analysis for phase diagrams

In this section, we explore the possible phase diagrams using RG analysis for the case where the two channels are degenerate, i.e., $J_1 = J_2 \equiv J$, $g_{\phi_1} = g_{\phi_2} \equiv \frac{1}{2}g_{\phi_\pm}$, and $K_1 = K_2 = J/T \equiv K$.

Due to the permutation symmetry between these two channels, the coupled theory is rewritten in terms of the collective basis $\theta_\pm$, $\phi_\pm$ channels conveniently defined as:

$$\begin{aligned}&\theta_+ \equiv (\theta_1+\theta_2)/2,\ \theta_- \equiv \theta_1-\theta_2,\\ &\phi_+ \equiv \phi_1+\phi_2, \qquad \phi_- \equiv (\phi_1-\phi_2)/2.\end{aligned} \tag{5}$$

The compact radius of $\theta_\pm$ can be chosen as 2π, and that of the vortex fields $\phi_\pm$ remains 1. This new basis is also convenient in the sense that it makes the symmetries of the coupled system explicit and at the same time it preserves the commutation relations between the fields and the dual fields, i.e., $[\theta_\pm(t,x), \partial_y\phi_\pm(t,y)] = 2\pi\mathrm{i}\delta(x-y)$. The Lagrangian has a $U(1)$ symmetry in θ_+ channel, $\theta_+ \to \theta_+ + \alpha$ with $\alpha \in [0, 2\pi)$, and the Z_2 symmetry in the θ_- channel, $\theta_- \to \theta_- + \pi$, due to the $\cos 2\theta_-$ term.

Based on symmetry alone, there can exit four different phases: (i) Both $U(1)$ and Z_2 are unbroken, i.e., the normal phase; (ii) only Z_2 is broken, i.e., TRS-breaking (or nematic) normal phase; (iii) only $U(1)$ is broken, i.e., the charge-$4e$ phase; (iv) both $U(1)$ and Z_2 are broken, i.e., the TRS-breaking (or nematic) superconducting phase. We can start with the free theory containing only the kinetic terms, and then add on the most relevant symmetry-preserving interaction terms to obtain phase diagrams containing all of the four possible phases discussed above, but with different phase diagram topologies.

With the basis transformation defined above, the free part of the Lagrangian in eq. (4) can be equivalently written in the $\theta_\pm, \phi_\pm$ basis as:

$$\mathcal{L}_0(x) = \frac{1}{4K_+}(\partial_\mu\phi_+)^2 + \frac{1}{K_-}(\partial_\mu\phi_-)^2, \tag{6}$$

where the initial values of both $K_\pm$ are both J/T.

Once various interaction terms are added, the phase diagram lives in a high dimensional parameter space. As a result, it is difficult to present a complete phase diagram involving all the parameters. However, based on the symmetry analysis provided above, there are only four phases in total. Therefore, it is possible to show two dimensional (2D) slices of the phase diagram that contains the four phases. Interestingly enough, topologically distinct configurations of phase boundaries can be obtained, depending on which interaction terms dominate at low energy. In the following two subsections, we will present two generic cases showing three types of phase diagram topologies.

4.1 $\phi_\pm$ channels decoupled

We consider possible local vortex terms in the collective basis, which are discussed in Appendix A3. The most relevant one is $g_{\phi_{\rm int}}\cos\pi\phi_+\cos 2\pi\phi_-$, which couples the even and odd channels together. It originates from the vortex fugacity terms in the individual basis $\cos 2\pi\phi_1 + \cos 2\pi\phi_2$. The sign change of $\cos\pi\phi_+\cos 2\pi\phi_-$ from shifting ϕ_+ by 1 can be compensated by a shift of ϕ_- by $1/2$, and *vice versa*. The next leading vortex terms are $g_{\phi_+}\cos 2\pi\phi_+$ and $g_{\phi_-}\cos 4\pi\phi_-$ in the even and odd channels, respectively, which originate from the inter-layer vortex-vortex coupling in the original basis $\cos 2\pi\phi_1\cos 2\pi\phi_2 \pm \sin 2\pi\phi_1 \sin 2\pi\phi_2$.

We begin with the limit that the initial value of the inter-layer phase coupling g_{θ_-} is large. In this case, vortices in two layers tend to be aligned together. Hence, the independent single vortex excitation in each layer is not favored and its fugacity is suppressed, i.e., $|g_{\phi_\pm}| \gg |g_{\phi_{\rm int}}|$. In this limit, the $g_{\phi_{\rm int}}$-term is neglected, then the system is decoupled in the collective basis with Lagrangian given by

$$\begin{aligned}\mathcal{L}_1(x) =& \frac{1}{4K_+}(\partial_\mu\phi_+)^2 + \frac{1}{K_-}(\partial_\mu\phi_-)^2\\ &- g_{\phi_+}\cos 2\pi\phi_+ - g_{\phi_-}\cos 4\pi\phi_- + g_{\theta_-}\cos 2\theta_-.\end{aligned} \tag{7}$$

In this decoupled case, we expect the $U(1)$-breaking transition in the θ_+ channel to be completely independent from the Z_2-breaking transition in the θ_- channel. The phase diagram can be obtained by numerically solving the following set of RG equations (see Appendix A2 for details),

$$\begin{aligned}\frac{\mathrm{d}g_{\phi_+}}{\mathrm{d}\ln l} &= (2-2\pi K_+)\,g_{\phi_+},\\ \frac{\mathrm{d}g_{\phi_-}}{\mathrm{d}\ln l} &= (2-2\pi K_-)\,g_{\phi_-},\\ \frac{\mathrm{d}g_{\theta_-}}{\mathrm{d}\ln l} &= \left(2-\frac{2}{\pi K_-}\right)g_{\theta_-},\\ \frac{\mathrm{d}K_+}{\mathrm{d}\ln l} &= -2\pi^3 g_{\phi_+}^2 K_+^2,\\ \frac{\mathrm{d}K_-}{\mathrm{d}\ln l} &= -4\pi^3 g_{\phi_-}^2 K_-^2 + 4\pi g_{\theta_-}^2,\end{aligned} \tag{8}$$

where both of the initial values of $K_\pm$ are J/T.

Below we analyze the nature of the fixed points of RG for four different phases: (I) the Z_2 breaking SC phase; (II) Z_2 breaking normal phase; (III) quartetting phase; (IV) normal phase. The values of couplings at these fixed points are summarized in Table 1.

Phase I and Phase II are the Z_2 breaking superconducting (SC) and normal phases, respectively. In the former case, the relative phase θ_- is locked, while the θ_+ is quasi-long-range ordered. Hence, $g_{\theta_-} \to \infty$ and correspondingly $K_- \to \infty$. As for the vortex term $\cos 2\pi\phi_+$ in the ϕ_+ channel, such a vortex term should be irrelevant in Phase I, which requires that K_+ takes a constant value with $K_+ > 1/\pi$, and $(g_{\phi_-}, g_{\phi_+}) \to (0,0)$. In the Z_2-breaking normal phase, the relative phase θ_- remains locked, while the vortex ϕ_+ proliferates such that superfluidity is lost. Notice that the Z_2-breaking normal state appears in the intermediate temperature, i.e., the phase fluctuations of the underlying SC state lead to the symmetry-breaking normal state above the SC critical temperature. This intermediate phase can be the TRS breaking state, or, the nematic state depending on the θ_- is pinned at $\pm\frac{\pi}{2}$, or, 0 or π, respectively. In such a phase, $g_{\theta_-} \to \infty$ and $K_- \to +\infty$, which are the same as in Phase I. On the other hand, in order to proliferate vortices in the ϕ_+ channel, $g_{\phi_+} \to \infty$, which means $K_+ \to 0$. Then $(g_{\phi_-}, g_{\phi_+}) \to (0, \infty)$.

Phase III and Phase IV, i.e., the quartetting ($4e$) state and the normal state, are both the Z_2-symmetric phases. For the quartetting ($4e$) state, the vortex field in the relative channel ϕ_- condenses, while the θ_+ channel is quasi-long-range ordered. The condensation of ϕ_- means that $g_{\theta_-} \to 0$ and $K_- \to 0$, and $g_{\phi_-} \to \infty$. The quasi-long-range ordering of θ_+ requires $g_{\phi_+} \to 0$, which means that the renormalized value of K_+ reaches a constant with $K_+ > \frac{1}{\pi}$, which becomes a line of stable fixed points. As for the normal state, it means that the vortex fields in both channels condense. This simply gives rise to $g_{\phi_+} \to \infty$, $g_{\phi_-} \to \infty$, and $g_{\theta_-} \to 0$, which corresponds to $K_+ \to 0$ and $K_- \to 0$.

By numerically integrating the RG eq. (8), the above four phases are obtained. The phase diagram as a function of temperature and fugacity ratio between two channels g_{ϕ_-}/g_{ϕ_+} is shown in Figure 1. The fixed point values of the couplings deep in the four phases as well as on the phase boundaries are listed in Table 1. As expected, when the two channels are decoupled, the $U(1)$-breaking phase boundary and the Z_2-breaking phase boundary are independent from each other and cross at a single point, diving the phase diagram into four regions characterized by different symmetry breaking patterns.

Along the phase boundary P_1P_3 (excluding the multi-critical point O), it represents a Z_2-breaking transition inside the normal state with $K_- = \frac{1}{\pi}$. Then the fixed point condition for K_- can be solved to give the relation $|g_{\phi_-}| = |g_{\theta_-}|$. The segment of P_1O lies in the normal state with $g_{\phi_+} = \infty$ with $K_+ \to 0$ separating the Z_2-breaking normal state and the complete normal state. In contrast, the P_3O lies in the region with quasi-long-range ordered $U(1)$ phase θ_+ separating the Z_2-breaking SC state with θ_- locked and the quartetting charge-$4e$ phase. The boundary of P_2P_4 separates the superfluid phase and the normal phase, below which the $U(1)$ phase θ_+ becomes quasi-long-range ordered. The line of P_2O marks the boundary between the Z_2-breaking normal and SC phases. Similarly, the line of P_4O marks the boundary between the quartetting phase and the normal phase.

Here we comment on the exact duality on the critical line P_1P_3. More precisely, it is the duality between the field θ_- and its dual ϕ_-. To make the duality manifest, we can do a field rescaling

$$\tilde{\phi}_- \equiv \sqrt{2\pi}\phi_-, \quad \tilde{\theta}_- \equiv \theta_-/\sqrt{2\pi}, \tag{9}$$

such that the two mass terms become $\cos\sqrt{8\pi}\tilde{\phi}_-$ and $\cos\sqrt{8\pi}\tilde{\theta}_-$ respectively. At the same time, the Luttinger

Table 1 Values of couplings at fixed points in the four phases and on phase boundaries under RG eq. (8)

Phases and phase boundaries	g_{θ_-}	g_{ϕ_-}	g_{ϕ_+}	K_-	K_+
(I) Z_2-breaking SC	∞	0	0	$+\infty$	$> \frac{1}{\pi}$
(II) Z_2-breaking normal	∞	0	∞	$+\infty$	0
(III) quartetting ($4e$)	0	∞	0	0	$> \frac{1}{\pi}$
(IV) normal	0	∞	∞	0	0
P_1O	$\frac{g_{\phi_-}}{g_{\theta_-}} = \pm 1$		∞	$\frac{1}{\pi}$	0
P_2O	∞	0	0	$+\infty$	$\frac{1}{\pi}$
P_3O	$\frac{g_{\phi_-}}{g_{\theta_-}} = \pm 1$		0	$\frac{1}{\pi}$	$\frac{1}{\pi}$
P_4O	0	∞	0	0	$\frac{1}{\pi}$

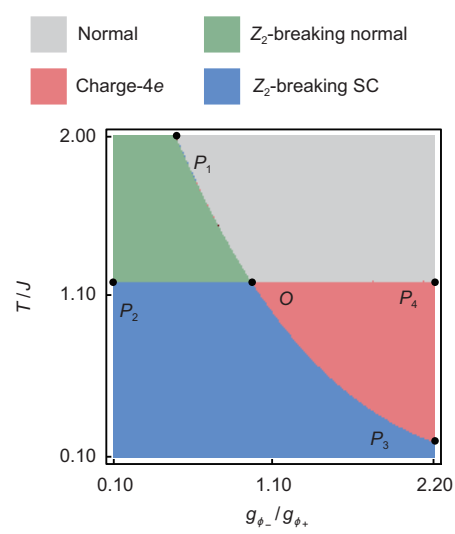

Figure 1 (Color online) Phase diagram vs. temperature and g_{ϕ_-}/g_{ϕ_+} by numerically integrating the RG eq. (8). The initial values of coupling constants are $g_{\phi_+} = 0.2$ and $g_{\theta_-} = 0.01$. All of the four phases appear and meet at the multi-cirtical point O.

parameter also has to be rescaled $\tilde{K}_- \equiv \pi K_-$, which becomes 1 at the critical point. It is again straightforward to show that $|g_{\phi_-}| = |g_{\theta_-}|$ at criticality. Then the duality of exchanging $\tilde{\theta}_-$ and $\tilde{\phi}_-$ on the Lagrangian level is made explicit. Such a theory has also been studied as the field theory description of one dimensional deconfined quantum critical point with $Z_2 \times Z_2$ symmetry [61]. In our case, the first Z_2 acts on the field θ_-, and the second Z_2 acts on its dual ϕ_-. The mixed anomaly between the two Z_2 symmetries dictates that when one is preserved the other has to be spontaneously broken. It has also been shown that such exotic critical point can be mapped to the usual Landau symmetry-breaking transition of a 1D Z_4 clock model, whose critical point is just two decoupled copies of Ising CFT [61,62]. It is interesting to note that such exotic critical point can arise naturally in the two-gap superconductors that we study.

4.2 $\phi_\pm$ coupled through $\cos\pi\phi_+ \cos 2\pi\phi_-$

Now we add the vortex term of $\cos\pi\phi_+ \cos 2\pi\phi_-$ which couples the $\phi_\pm$ fields together. The following Lagrangian is obtained:

$$\begin{aligned}\mathcal{L}_2(x) =& \frac{1}{K_-}(\partial_\mu\phi_-)^2 + \frac{1}{4K_+}(\partial_\mu\phi_+)^2 \\ &+ g_{\theta_-}\cos 2\theta_- - g_{\phi_{\rm int}}\cos\pi\phi_+\cos 2\pi\phi_- \\ &- g_{\phi_-}\cos 4\pi\phi_- - g_{\phi_+}\cos 2\pi\phi_+. \end{aligned} \tag{10}$$

The RG equations can be written down as the following (see Appendix A2):

$$\begin{aligned}\frac{\mathrm{d}g_{\theta_-}}{\mathrm{d}\ln l} &= \left(2 - \frac{2}{\pi K_-}\right) g_{\theta_-}, \\ \frac{\mathrm{d}g_{\phi_{\rm int}}}{\mathrm{d}\ln l} &= \left[2 - \frac{\pi}{2}(K_+ + K_-)\right] g_{\phi_{\rm int}}, \\ \frac{\mathrm{d}K_-}{\mathrm{d}\ln l} &= -4\pi^3 K_-^2\left(g_{\phi_-}^2 + g_{\phi_{\rm int}}^2/8\right) + 4\pi g_{\theta_-}^2 \\ \frac{\mathrm{d}K_+}{\mathrm{d}\ln l} &= -4\pi^3 K_+^2\left(g_{\phi_+}^2 + g_{\phi_{\rm int}}^2/8\right), \\ \frac{\mathrm{d}g_{\phi_-}}{\mathrm{d}\ln l} &= (2 - 2\pi K_-)\, g_{\phi_-} + \frac{\pi}{4} g_{\phi_{\rm int}}^2, \\ \frac{\mathrm{d}g_{\phi_+}}{\mathrm{d}\ln l} &= (2 - 2\pi K_+)\, g_{\phi_+} + \frac{\pi}{4} g_{\phi_{\rm int}}^2. \end{aligned} \tag{11}$$

By analyzing eq. (11), again we have the four stable phases as discussed in the decoupled case in the previous section before. The values of couplings at the fixed points corresponding to these phases and at the phase boundaries are summarized in Table 2. Compared with the decoupled case, the Z_2-breaking SC phase, the Z_2-breaking normal phase, and the quartetting phase further require that $g_{\phi_{\rm int}} \to 0$. Furthermore, the quartetting phase requires $K_+ > \frac{4}{\pi}$ to ensure the irrelevancy of the $g_{\phi_{\rm int}}$-term. As for the normal phase, certainly $g_{\phi_{\rm int}} \to \infty$.

A key feature of the new phase diagram after introducing the $g_{\phi_{\rm int}}$ term is that the previous tetra-critical point O splits into a pair of tri-critical points O_1 and O_2, such that there appears a direct transition across O_1O_2 from the Z_2-breaking SC phase to the normal state [63].

A small $g_{\phi_{\rm int}}$-term does not change the boundaries much when deep inside the Z_2-ordered or the superconducting regions as long as they are relatively far away from O_1O_2. In this case, the RG processes in the two channels can be decomposed into fast and slow steps. For example, along the boundary P_2O_1 deep inside the Z_2-breaking phase, θ_- is pinned, which renders the $g_{\phi_{\rm int}}$-term highly irrelevant by disordering the ϕ_- field. Similarly, along the boundary P_3O_2 deep inside the superfluid phase, g_{ϕ_+} is quickly suppressed to 0. The RG process in the ϕ_+ channel stops quickly, such that $g_{\phi_{\rm int}}$ does not grow much and remains small still. Furthermore, ϕ_+ remains power-law fluctuating, which suppresses the effect of the $g_{\phi_{\rm int}}$-term.

On the other hand, the $g_{\phi_{\rm int}}$-term affects the boundaries surrounding the normal phase. As for the part along P_4O_1 deep inside the Z_2-disordered region, ϕ_- is pinned. The $g_{\phi_{\rm int}}$-term becomes $g'\cos\pi\phi_+$, which is a half-quantum vortex with a renormalized coupling constant $g' = g_{\phi_{\rm int}}\langle\cos 2\pi\phi_-\rangle$. Such a term is more relevant than the one-vortex term of $g_{\phi+}$ although its coupling is weaker. Nevertheless, it extends the region of the normal state significantly as shown in Figure 2. As for P_1O_1 deep inside the normal phase, g_{ϕ_+}-term reaches the order of 1 quickly, and ϕ_+ is pinned. Then the $g_{\phi_{\rm int}}$-term becomes $g''\cos 2\pi\phi_-$ with $g'' = g_{\phi_{\rm int}}\langle\cos\pi\phi_+\rangle$, which is more relevant than the existing $g_{\phi_-}\cos 4\pi\phi_-$ term. It changes the competition between the condensation of θ_- and ϕ_-, which corresponds to the Z_2-ordered and disordered state, respectively. The critical theory on P_1O_1 is also modified as a consequence of the $g_{\phi_{\rm int}}$-term. Based on the numerical solution near this critical line, the

Table 2 The values of couplings at the fixed points corresponding to four stable phases and on the phase boundaries by solving eq. (11)

Phases	g_{θ_-}	g_{ϕ_-}	$g_{\phi+}$	$g_{\phi_{\rm int}}$	K_+	K_-
(I) Z_2-breaking SC	∞	0	0	0	$> \frac{1}{\pi}$	$+\infty$
(II) Z_2-breaking normal	∞	0	∞	0	0	$+\infty$
(III) Quartetting (4e)	0	∞	0	0	$> \frac{4}{\pi}$	0
(IV) Normal	0	∞	∞	∞	0	0
P_1O_1	∞	∞	∞	∞	0	$\frac{1}{\pi}$
P_2O_1	∞	0	0	0	$\frac{1}{\pi}$	0
P_3O_2	$\frac{g_{\phi_-}}{g_{\theta_-}} = \pm 1$		0	0	$> \frac{4}{\pi}$	$\frac{1}{\pi}$
P_4O_2	0	∞	0	0	$\frac{1}{\pi}$	0
O_1O_2	$\frac{g_{\phi_-}}{g_{\theta_-}} = \pm 1$		0	0	$\frac{1}{\pi}$	$\frac{1}{\pi}$

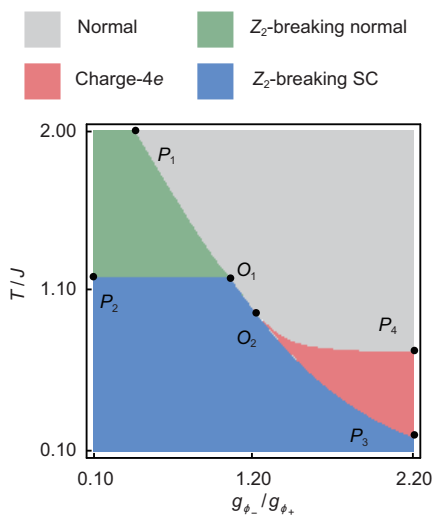

Figure 2 (Color online) Phase diagram vs. temperature and g_{ϕ_-}/g_{ϕ_+} by numerically integrating the RG eq. (11). The initial values of coupling constants are $g_{\phi_+} = 0.2, g_{\theta_-} = 0.01$ and $g_{\phi_{\rm int}} = 0.001$. Different from Figure 1, this phase diagram features a direct transition boundary O_1O_2 between the normal state and the Z_2-breaking SC phase due to the coupling between the $\phi_\pm$ channels.

scaling dimensions of the two competing interaction terms, the $g_{\phi_{\rm int}}$-term and the g_{θ_-}-term both stabilize at 1, indicating the criticality belongs to the Ising universality class. In contrast, the critical behavior on P_3O_1 for the θ_--channel inherits from the critical line P_3O in Figure 1 since $g_{\phi_{\rm int}}$ flows to 0 and this coupling term is non-consequential.

When close to O_1O_2, the energy scales in the even and odd channels are close, hence, the RG processes cannot be decomposed into fast and slow steps any more. Since the $g_{\phi_{\rm int}}$-term is the most relevant, it grows quickly and overwhelms other terms under sufficiently long RG processes. Once $g_{\phi_{\rm int}}$ is renormalized to the strong coupling region, both ϕ_+ and ϕ_- are pinned, thus the system enters into normal state. Once it is renormalized to zero, the system is in the SC state and the residual g_{θ_-}-term will drive the Z_2 symmetry breaking. The transitions on the critical lines across the tri-critical points O_1 and O_2 are also quite interesting, but we leave the details for future study.

5 Discussion

We briefly discuss the application of our theory to the $FeTe_{1-x}Se_x$ superconductor, in which evidence to spontaneously time-reversal-symmetry breaking states has been observed by using the high-resolution laser-based photoemission method both in the superconducting and the normal states [41].

Following ref. [64], we consider two superconducting gap functions Δ_1 and Δ_2, which possess different pairing symmetries and each of them maintains time-reversal symmetry. It has been argued that the pairing symmetries are constrained to be among $A_{1g(u)} \pm {\rm i}A_{2g(u)}$, $B_{1g(u)} \pm {\rm i}B_{2g(u)}$, or $E_{g(u)} \pm {\rm i}E_{g(u)}$, based on the effects of TRS-breaking pairing on the surface Dirac cone. Here A, B, E denote discrete angular momenta analogous to the s, d, p-wave in the continuous case. g and u denote even and odd parities respectively. $A_{1,2}$ means even or odd under vertical plane reflection. The Ginzburg-Landau free energy is given by

$$\begin{aligned}\mathcal{F} =&\alpha_1|\Delta_1|^2 + \beta_1|\Delta_1|^4 + \alpha_2|\Delta_2|^2 + \beta_2|\Delta_2|^4 \\ &+ \kappa|\Delta_1|^2|\Delta_2|^2 + \lambda\left((\Delta_1^*\Delta_2)^2 + c.c.\right),\end{aligned} \tag{12}$$

where $\alpha_1 \approx \alpha_2$ is assumed so that the two pairing channels are nearly degenerate as discussed before. And we focus on the case of $\lambda > 0$, where the relative phase between Δ_1 and Δ_2 as $\theta_- = \pm\frac{\pi}{2}$. Hence, the complex gap function $\Delta_1 \pm {\rm i}\Delta_2$ spontaneously breaks time-reversal symmetry.

Since the $FeSe_{1-x}Te_x$ superconductor has strong atomic spin-orbit coupling, as allowed by symmetry, the complex gap function can directly couple to the spin magnetization m_z via a cubic coupling term as:

$$\mathcal{F}_M = \alpha_m|m_z|^2 + {\rm i}\gamma m_z(\Delta_1\Delta_2^* - \Delta_1^*\Delta_2), \tag{13}$$

where $\alpha_m > 0$ and γ is proportional to the spin-orbit coupling strength [64]. This term satisfies both the $U(1)$ symmetry and time-reversal symmetry. Because of $\alpha_m > 0$, the spin magnetization can only be induced by the complex gap function via $m_z = \frac{\gamma}{\alpha_m}|\Delta_1^*\Delta_2|\sin\theta_-$ when $\theta_- = \pm\frac{\pi}{2}$. The development of m_z will gap out the surface Dirac cone as observed in the experiment [41]. As detailed in ref. [64], this spontaneous breaking of TR symmetry can impose a strong constraint on the gap function symmetry in the $FeSe_{1-x}Te_x$ system.

Furthermore, recent experiment [41] also shows that the spin-magnetization develops nonzero values even at $T > T_c$, indicating that TRS breaking already occurs above T_c. It can be understood from the analysis in the main text, where we propose the Z_2-breaking normal state. There are no long-range superconducting orderings, i.e., the $\langle\Delta_1\rangle = \langle\Delta_2\rangle = 0$. However, the expectation value of the 4-fermion order parameter is nonzero $\langle\Delta_1^*\Delta_2\rangle \neq 0$ due to the pinning of $\theta_- = \pm\frac{\pi}{2}$.

6 Conclusions

To summarize, we have analyzed the possible symmetry-breaking phases in the phase fluctuation regime in a two-gap superconductors in 2D. The system has an overall $Z_2 \times U(1)$ symmetry, where the Z_2 in the θ_- channel is due to the second order Josephson coupling between the two gaps and the θ_+ channel still has $U(1)$ symmetry. If only the Z_2 is broken, then we have the Z_2-breaking normal state, which can

be either the phase fluctuation induced TRS breaking normal state or the nematic state, depending on whether the relative phase θ_- is locked at $\pm\frac{\pi}{2}$, or, at 0 or π. On the other hand, if only the $U(1)$ symmetry is broken, then it corresponds to the ordering of the total phase θ_+, even though the two gaps are not individually ordered. This is the quartetting phase, or the so-called 4*e* phase.

Extensive RG analysis is done by including the more relevant symmetry allowed couplings. Not only have we obtained all the four possible phases, including the two interesting intermediate phases in the phase fluctuation regime, we also find a direct transition from the Z_2-breaking SC state to the normal state. This is because the coupling between half-vortices in the even and odd channels favors the simultaneous ordering/disordering of the two channels.

On the experimental side, the TRS-breaking normal phase has been experimentally observed recently in hole-doped $Ba_{1-x}K_xFe_2As_2$ [49, 50]. Furthermore, experimental evidence of the elusive charge-4*e* state has also been found recently in kagome superconductor CsV_3Sb_5 [52]. The theory presented in this work is based on general symmetry principles. We believe the fluctuation effects and the physical consequences discussed here are quite generic and likely play a role in a wide range of multi-gap superconductors with dominant second-order Josephson couplings.

Note added: Upon the completion of the first version of this manuscript, we became aware of two manuscripts on related topics refs. [65,66]. Very recently, similar physics have also been discussed in ref. [67].

We thank Fan Yang, Yu-Bo Liu, and Jing Zhou for helpful discussions. Meng Zeng, Hong-Ye Hu, and Yi-Zhuang You are supported by a startup funding of UCSD and the National Science Foundation (Grant No. DMR-2238360). Congjun Wu is supported by the National Natural Science Foundation of China (Grant Nos. 12234016, and 12174317). This work has been supported by the New Cornerstone Science Foundation.

Conflict of interest The authors declare that they have no conflict of interest.

1 J. G. Bednorz, and K. A. Müller, Z. Phys. B-Condensed Matter **64**, 189 (1986).
2 G. R. Stewart, Rev. Mod. Phys. **56**, 755 (1984).
3 H. Takahashi, K. Igawa, K. Arii, Y. Kamihara, M. Hirano, and H. Hosono, Nature **453**, 376 (2008).
4 W. C. Lee, S. C. Zhang, and C. Wu, Phys. Rev. Lett. **102**, 217002 (2009), arXiv: 0810.0887.
5 C. Wu, and J. E. Hirsch, Phys. Rev. B **81**, 020508 (2010).
6 V. Stanev, and Z. Tešanović, Phys. Rev. B **81**, 134522 (2010), arXiv: 0912.5214.
7 M. Khodas, and A. V. Chubukov, Phys. Rev. Lett. **108**, 247003 (2012), arXiv: 1202.5563.
8 J. Garaud, and E. Babaev, Phys. Rev. Lett. **112**, 017003 (2014), arXiv: 1308.3220.
9 S. Maiti, M. Sigrist, and A. Chubukov, Phys. Rev. B **91**, 161102 (2015), arXiv: 1412.7439.
10 S. Z. Lin, S. Maiti, and A. Chubukov, Phys. Rev. B **94**, 064519 (2016), arXiv: 1607.00109.
11 Y. Wang, and L. Fu, Phys. Rev. Lett. **119**, 187003 (2017), arXiv: 1703.06880.
12 J. Kang, A. V. Chubukov, and R. M. Fernandes, Phys. Rev. B **98**, 064508 (2018), arXiv: 1805.06882.
13 Z. Wang, G. M. Zhang, Y. Yang, and F. C. Zhang, Phys. Rev. B **102**, 220501 (2020), arXiv: 2006.15928.
14 L. H. Hu, P. D. Johnson, and C. Wu, Phys. Rev. Res. **2**, 022021 (2020), arXiv: 1906.01754.
15 R. B. Laughlin, Phys. Rev. Lett. **80**, 5188 (1998), arXiv: cond-mat/9709004.
16 S. Tewari, C. Zhang, V. M. Yakovenko, and S. Das Sarma, Phys. Rev. Lett. **100**, 217004 (2008), arXiv: 0711.2329.
17 Y. Wang, M. Lin, and T. L. Hughes, Phys. Rev. B **98**, 165144 (2018), arXiv: 1804.01531.
18 C. Platt, R. Thomale, C. Honerkamp, S. C. Zhang, and W. Hanke, Phys. Rev. B **85**, 180502 (2012), arXiv: 1106.5964.
19 W. Yang, C. Xu, and C. Wu, Phys. Rev. Res. **2**, 042047 (2020).
20 M. Silaev, J. Garaud, and E. Babaev, Phys. Rev. B **95**, 024517 (2017), arXiv: 1610.05846.
21 R. P. Singh, A. D. Hillier, B. Mazidian, J. Quintanilla, J. F. Annett, D. M. K. Paul, G. Balakrishnan, and M. R. Lees, Phys. Rev. Lett. **112**, 107002 (2014), arXiv: 1401.2108.
22 G. M. Pang, Z. Y. Nie, A. Wang, D. Singh, W. Xie, W. B. Jiang, Y. Chen, R. P. Singh, M. Smidman, and H. Q. Yuan, Phys. Rev. B **97**, 224506 (2018), arXiv: 1806.03768.
23 J. A. Sauls, Adv. Phys. **43**, 113 (1994), arXiv: 1812.09984.
24 E. R. Schemm, W. J. Gannon, C. M. Wishne, W. P. Halperin, and A. Kapitulnik, Science **345**, 190 (2014), arXiv: 1410.1482.
25 Y. Aoki, A. Tsuchiya, T. Kanayama, S. R. Saha, H. Sugawara, H. Sato, W. Higemoto, A. Koda, K. Ohishi, K. Nishiyama, and R. Kadono, Phys. Rev. Lett. **91**, 067003 (2003), arXiv: cond-mat/0308196.
26 A. P. MacKenzie, and Y. Maeno, Rev. Mod. Phys. **75**, 657 (2003).
27 E. R. Schemm, R. E. Baumbach, P. H. Tobash, F. Ronning, E. D. Bauer, and A. Kapitulnik, Phys. Rev. B **91**, 140506 (2015), arXiv: 1410.1479.
28 P. K. Biswas, H. Luetkens, T. Neupert, T. Stürzer, C. Baines, G. Pascua, A. P. Schnyder, M. H. Fischer, J. Goryo, M. R. Lees, H. Maeter, F. Brückner, H. H. Klauss, M. Nicklas, P. J. Baker, A. D. Hillier, M. Sigrist, A. Amato, and D. Johrendt, Phys. Rev. B **87**, 180503 (2013).
29 A. D. Hillier, J. Quintanilla, and R. Cywinski, Phys. Rev. Lett. **102**, 117007 (2009), arXiv: 0901.3153.
30 A. D. Hillier, J. Quintanilla, B. Mazidian, J. F. Annett, and R. Cywinski, Phys. Rev. Lett. **109**, 097001 (2012), arXiv: 1206.5905.
31 Z. F. Weng, J. L. Zhang, M. Smidman, T. Shang, J. Quintanilla, J. F. Annett, M. Nicklas, G. M. Pang, L. Jiao, W. B. Jiang, Y. Chen, F. Steglich, and H. Q. Yuan, Phys. Rev. Lett. **117**, 027001 (2016), arXiv: 1605.08356.
32 X. Gong, M. Kargarian, A. Stern, D. Yue, H. Zhou, X. Jin, V. M. Galitski, V. M. Yakovenko, and J. Xia, Sci. Adv. **3**, e1602579 (2017), arXiv: 1609.08538.
33 T. Shang, M. Smidman, A. Wang, L. J. Chang, C. Baines, M. K. Lee, Z. Y. Nie, G. M. Pang, W. Xie, W. B. Jiang, M. Shi, M. Medarde, T. Shiroka, and H. Q. Yuan, Phys. Rev. Lett. **124**, 207001 (2020), arXiv: 2004.10425.
34 S. K. Ghosh, M. Smidman, T. Shang, J. F. Annett, A. D. Hillier, J. Quintanilla, and H. Yuan, J. Phys.-Condens. Matter **33**, 033001 (2021), arXiv: 2003.04357.
35 A. Schenck, *Muon Spin Rotation Spectroscopy: Principles and Applications in Solid State Physics* (Taylor and Francis, London, 1985).
36 S. L. Lee, R. Cywinski, and S. Kilcoyne, *Muon Science: Muons in Physics, Chemistry and Materials*, volume 51 (CRC Press, Boca Raton, 1999).
37 A. Yaouanc, and P. D. De Reotier, *Muon Spin Rotation, Relaxation, and Resonance: Applications to Condensed Matter*, volume 147 (Oxford University Press, Oxford, 2011).
38 S. Spielman, K. Fesler, C. B. Eom, T. H. Geballe, M. M. Fejer, and A.

Kapitulnik, Phys. Rev. Lett. **65**, 123 (1990).
39 A. Kapitulnik, J. Xia, E. Schemm, and A. Palevski, New J. Phys. **11**, 055060 (2009), arXiv: 0906.2845.
40 V. Grinenko, R. Sarkar, K. Kihou, C. H. Lee, I. Morozov, S. Aswartham, B. Büchner, P. Chekhonin, W. Skrotzki, K. Nenkov, R. Hühne, K. Nielsch, S. L. Drechsler, V. L. Vadimov, M. A. Silaev, P. A. Volkov, I. Eremin, H. Luetkens, and H. H. Klauss, Nat. Phys. **16**, 789 (2020).
41 N. Zaki, G. Gu, A. Tsvelik, C. Wu, and P. D. Johnson, Proc. Natl. Acad. Sci. U.S.A. **118**, e2007241118 (2021).
42 V. J. Emery, and S. A. Kivelson, Nature **374**, 434 (1995).
43 S. Kasahara, T. Yamashita, A. Shi, R. Kobayashi, Y. Shimoyama, T. Watashige, K. Ishida, T. Terashima, T. Wolf, F. Hardy, C. Meingast, H. Löhneysen, A. Levchenko, T. Shibauchi, and Y. Matsuda, Nat. Commun. **7**, 12843 (2016), arXiv: 1608.01829.
44 Z. Cai, and C. Wu, Phys. Rev. A **84**, 033635 (2011), arXiv: 1106.1121.
45 F. Hébert, Z. Cai, V. G. Rousseau, C. Wu, R. T. Scalettar, and G. G. Batrouni, Phys. Rev. B **87**, 224505 (2013), arXiv: 1304.0554.
46 T. A. Bojesen, E. Babaev, and A. Sudbø, Phys. Rev. B **88**, 220511 (2013), arXiv: 1306.2313.
47 C. Wu, Phys. Rev. Lett. **95**, 266404 (2005), arXiv: cond-mat/0409247.
48 E. Berg, E. Fradkin, and S. A. Kivelson, Nat. Phys. **5**, 830 (2009), arXiv: 0904.1230.
49 V. Grinenko, D. Weston, F. Caglieris, C. Wuttke, C. Hess, T. Gottschall, I. Maccari, D. Gorbunov, S. Zherlitsyn, J. Wosnitza, A. Rydh, K. Kihou, C. H. Lee, R. Sarkar, S. Dengre, J. Garaud, A. Charnukha, R. Hühne, K. Nielsch, B. Büchner, H. H. Klauss, and E. Babaev, Nat. Phys. **17**, 1254 (2021).
50 I. Shipulin, N. Stegani, I. Maccari, K. Kihou, C.-H. Lee, Y. Li, R. Hhne, H.-H. Klauss, M. Putti, F. Caglieris, E. Babaev, and V. Grinenko, arXiv: 2212.13515.
51 R. Russell, H. P. Nair, K. M. Shen, D. G. Schlom, and J. W. Harter, arXiv: 2304.02586.
52 J. Ge, P. Wang, Y. Xing, Q. Yin, H. Lei, Z. Wang, and J. Wang, arXiv: 2201.10352.
53 M. Cheng, K. Sun, V. Galitski, and S. Das Sarma, Phys. Rev. B **81**, 024504 (2010), arXiv: 0908.2805.
54 C. Wu, Mod. Phys. Lett. B **23**, 1 (2009), arXiv: 0901.1415.
55 F. Hébert, Z. Cai, V. G. Rousseau, C. Wu, R. T. Scalettar, and G. G. Batrouni, Phys. Rev. B **87**, 224505 (2013), arXiv: 1304.0554.
56 R. M. Fernandes, P. P. Orth, and J. Schmalian, Annu. Rev. Condens. Matter Phys. **10**, 133 (2019), arXiv: 1804.00818.
57 M. H. Fischer, and E. Berg, Phys. Rev. B **93**, 054501 (2016), arXiv: 1511.05177.
58 C. Wu, W. V. Liu, and E. Fradkin, Phys. Rev. B **68**, 115104 (2003), arXiv: cond-mat/0206248.
59 L. H. Hu, R. X. Zhang, F. C. Zhang, and C. Wu, Phys. Rev. B **102**, 235115 (2020), arXiv: 1912.09066.
60 E. Fradkin, *Field Theories of Condensed Matter Physics* (Cambridge University Press, Cambridge, 2013).
61 C. Zhang, and M. Levin, Phys. Rev. Lett. **130**, 026801 (2023), arXiv: 2206.01222.
62 L. Su, arXiv: 2306.02976.
63 F. F. Song, and G. M. Zhang, Phys. Rev. Lett. **128**, 195301 (2022), arXiv: 2105.05411.
64 L. H. Hu, P. D. Johnson, and C. Wu, Phys. Rev. Res. **2**, 022021 (2020), arXiv: 1906.01754.
65 R. M. Fernandes, and L. Fu, arXiv: 2101.07943.
66 S.-K. Jian, Y. Huang, and H. Yao, arXiv: 2102.02820.
67 Y.-B. Liu, J. Zhou, C. Wu, and F. Yang, arXiv: 2301.06357.
68 I. Herbut, *A Modern Approach to Critical Phenomena* (Cambridge University Press, Cambridge, 2007).
69 R. Shankar, *Quantum Field Theory and Condensed Matter: An Introduction* (Cambridge University Press, Cambridge, 2017).
70 A. M. Tsvelik, *Quantum Field Theory in Condensed Matter Physics* (Cambridge University Press, Cambridge, 2007).

Appendix

A1 The 2D classical XY-model and its dual to the sine-Gordon model

In this section, we review the duality transformation from the XY-model to the sine-Gordon model. We follow ref. [68] to review the duality between the XY-model and the sine-Gordon model. The Hamiltonian of a single-component XY-model with the coupling constant J is given by

$$H_{XY} = -J \sum_{\langle i,j \rangle} \cos(\theta_i - \theta_j). \tag{a1}$$

To map the XY-model to the sine-Gordon model, we start with the Villain approximation,

$$\mathrm{e}^{-K(1-\cos\theta)} \approx \sum_{n=-\infty}^{\infty} \mathrm{e}^{-\frac{K}{2}(\theta-2n\pi)^2}, \tag{a2}$$

which is valid when K is large. In this case, the dominant contribution comes from the regime that $\cos\theta \approx 1$, i.e., $\theta \approx 2n\pi$. Performing Taylor expansion around each of these values, we have $\mathrm{e}^{-K(1-\cos\theta)} \approx \sum_n \mathrm{e}^{-\frac{K}{2}(\theta-2n\pi)^2}$.

Using the Villain approximation, the Partition function of the XY-model in eq. (a1) is given by

$$\begin{aligned} Z_{XY} &= \int_0^{2\pi} \prod_i \frac{\mathrm{d}\theta_i}{2\pi} \mathrm{e}^{-\beta H_{XY}} = \int_0^{2\pi} \prod_i \frac{\mathrm{d}\theta_i}{2\pi} \mathrm{e}^{\beta J \sum_{\langle i,j \rangle} \cos(\theta_i - \theta_j)} \\ &= \int_0^{2\pi} \prod_i \frac{\mathrm{d}\theta_i}{2\pi} \prod_{\langle i,j \rangle} \sum_{m_{ij}} \mathrm{e}^{-K/2(\theta_i-\theta_j-2m_{ij}\pi)^2}, \end{aligned} \tag{a3}$$

where $K = \beta J = J/T$ and the Boltzmann constant is set to be 1 for simplicity; m_{ij} are integers defined on each link of the 2D lattice. Now we perform the Hubbard-Stratonovich transformation by introducing the continuous variables x_{ij} defined on each link of the lattice. The Partition function becomes

$$\begin{aligned} Z_{XY} = &\int_0^{2\pi} \prod_i \frac{\mathrm{d}\theta_i}{2\pi} \int_{-\infty}^{\infty} \prod_{<ij>} \sqrt{\frac{2K}{\pi}} \mathrm{d}x_{ij} \\ &\times \prod_{\langle i,j \rangle} \sum_{m_{ij}} \mathrm{e}^{-\frac{1}{2K}x_{ij}^2 - \mathrm{i}x_{ij}(\theta_i-\theta_j-2m_{ij}\pi)}. \end{aligned} \tag{a4}$$

With the help of the Poisson resummation formula,

$$\sum_n \delta(x - nT) = \sum_m \frac{1}{T} \mathrm{e}^{\mathrm{i}\frac{2m\pi}{T}x}, \tag{a5}$$

where n is an integer, the partition function Z_{XY} becomes

$$\begin{aligned} Z_{XY} = &\int_0^{2\pi} \prod_i \frac{\mathrm{d}\theta_i}{2\pi} \int_{-\infty}^{\infty} \prod_{<ij>} \sqrt{\frac{2K}{\pi}} \mathrm{d}x_{ij} \\ &\times \prod_{\langle i,j \rangle} \mathrm{e}^{-\frac{1}{2K}x_{ij}^2 - \mathrm{i}x_{ij}(\theta_i-\theta_j)} \sum_n \delta(x_{ij} - n) \end{aligned}$$

$$\sim \int_0^{2\pi} \prod_i \frac{d\theta_i}{2\pi} \sum_{\{m_{ij}\}} \prod_{\langle i,j\rangle} e^{-\frac{1}{2K} m_{ij}^2 - i m_{ij}(\theta_i - \theta_j)}. \tag{a6}$$

To perform the above integrals, each θ_i is extracted from its neighbors,

$$Z_{XY} \sim \int_0^{2\pi} \prod_i \frac{d\theta_i}{2\pi} \sum_{\{m_{ij}\}} e^{-\frac{1}{2K}\sum_{i,\hat{\mu}} m_{i,\hat{\mu}}^2 - i\sum_{i,\hat{\mu}}(m_{i,\hat{\mu}} - m_{i,-\hat{\mu}})\theta_i}, \tag{a7}$$

where $\hat{\mu} = \hat{x}, \hat{y}$ denotes the lattice unit vectors along the bond directions. Now the angles θ_i can be integrated out,

$$Z_{XY} \sim \sum_{\{m_{ij}\}} e^{-\frac{1}{2K}\sum_{i,\hat{\mu}} m_{i,\hat{\mu}}^2} \prod_i \delta\left(\sum_{\hat{\mu}} (m_{i,\hat{\mu}} - m_{i,-\hat{\mu}})\right), \tag{a8}$$

where the δ-function here is the Kronecker δ.

Each integer m_{ij} defined on the link can be treated as a current flown into and out of the connected lattice sites, and the δ-function here basically says the current through each site is conserved. This conservation constraint is naturally satisfied if we define another set of integers $\{n_i\}$ at the sites of the dual lattice, i.e., the centers of the plaquettes of the original lattice,

$$\begin{aligned} m_{i,\hat{x}} &= n_{i+\hat{x}+\hat{y}} - n_{i+\hat{x}}, \\ m_{i,\hat{y}} &= n_{i+\hat{y}} - n_{i+\hat{x}+\hat{y}}, \\ m_{i-\hat{x},\hat{x}} &= n_{i+\hat{y}} - n_i, \\ m_{i-\hat{y},\hat{y}} &= n_i - n_{i+\hat{x}}. \end{aligned} \tag{a9}$$

With the new set of integers, the partition function now becomes,

$$Z_{XY} \sim \sum_{\{n_i\}} e^{-\frac{1}{2K}\sum_{i,\hat{\mu}}(n_{i+\hat{\mu}} - n_i)^2}. \tag{a10}$$

Comparing with the original partition function, we notice that the temperature has been inverted because $K \to 1/K$, and continuous variables has been replaced by integer variables. However, we can use Poisson summation to go back to continuous variables. Therefore,

$$\begin{aligned} Z_{XY} &\sim \int \prod_i d\phi_i \sum_{\{n_i\}} e^{-\frac{1}{2K}\sum_{i,\hat{\mu}}(\phi_{i,\hat{\mu}} - \phi_i)^2} \prod_i \delta(\phi_i - n_i) \\ &= \int \prod_i d\phi_i \sum_{\{n_i\}} e^{-\frac{1}{2K}\sum_{i,\hat{\mu}}(\phi_{i,\hat{\mu}} - \phi_i)^2 - i2\pi\sum_i n_i\phi_i}. \end{aligned} \tag{a11}$$

After adding the chemical potential term, the Partition function becomes

$$Z_{XY} \sim \int \prod_i d\phi_i \sum_{\{n_i\}} e^{-\frac{1}{2K}\sum_{i,\hat{\mu}}(\phi_{i,\hat{\mu}} - \phi_i)^2 - i2\pi\sum_i n_i\phi_i + \ln y \sum_i n_i^2}. \tag{a12}$$

Next we perform the summation over $\{n_i\}$ by using the following identity,

$$\begin{aligned} \sum_{\{n_i\}} e^{-i2\pi\sum_i n_i\phi_i + \ln y\sum_i n_i^2} &= \prod_i \sum_{n_i=0,\pm1,\ldots} y^{n_i^2} e^{-i2\pi n_i\phi_i} \\ &= \prod_i (1 + 2y\cos 2\pi\phi_i + O(y^2)) \\ &= e^{2y\sum_i \cos 2\pi\phi_i}. \end{aligned} \tag{a13}$$

The partition function eventually becomes the form of the sine-Gordon model,

$$Z_{XY} \sim \int \prod_i d\phi_i e^{-\frac{1}{2K}\sum_{i,\hat{\mu}}(\phi_{i,\hat{\mu}} - \phi_i)^2 + 2y\sum_i \cos 2\pi\phi_i}. \tag{a14}$$

A2 RG equations from operator product expansions

A2.1 Scaling dimensions

In this part we use the operator product expansion (OPE) to calculate the scaling dimensions of the coupling terms consisting of vertex operators of the form $\cos\beta\phi$ in the free bosonic field ϕ and the vertex operators $\cos\beta\theta$ in the dual field θ, based on the free Lagrangian $\mathcal{L}_0 = \frac{1}{2K}(\partial_\mu\phi)^2$. Notice that the Luttinger parameter K in the results presented below have to be accordingly scaled in order to be used for the theory in eq. (6).

We start with the correlation functions of the following vertex operators. Following the notation in ref. [69], the correlation function is given by

$$G_\beta(x-y) \equiv \langle e^{i\beta\phi(x)} e^{-i\beta\phi(y)}\rangle. \tag{a15}$$

By using the operator identity: $e^A e^B :=: e^{A+B} : e^{\langle AB + \frac{A^2+B^2}{2}\rangle}$, where $:\hat{O}:$ means normal ordering, we have

$$\begin{aligned} G_\beta(x-y) &= \langle : e^{i\beta(\phi(x)-\phi(y))} : \rangle e^{-\frac{\beta^2}{2}\langle(\phi(x)-\phi(y))^2\rangle} \\ &= e^{\beta\langle\phi(x)\phi(y) - \phi^2(x)\rangle} = \lim_{l\to 0}\left(\frac{l^2}{l^2 + (x-y)^2}\right)^{\frac{\beta^2 K}{4\pi}}, \end{aligned} \tag{a16}$$

where l is the short distance cutoff. The following fact is used to derive the above equation,

$$\langle\phi(x)\phi(y) - \phi^2(x)\rangle = -\frac{K}{2\pi}\ln\frac{l^2}{l^2 + (x-y)^2}. \tag{a17}$$

Similarly, we have for the dual field θ:

$$\langle\theta(x)\theta(y) - \theta^2(x)\rangle = -\frac{1}{2\pi K}\ln\frac{l^2}{l^2 + (x-y)^2}. \tag{a18}$$

Therefore, we are able to obtain the following correlation functions for two different types of vertex operators:

$$\begin{aligned} \langle e^{i\beta\phi(x)} e^{-i\beta\phi(y)}\rangle &\sim |x-y|^{-\frac{\beta^2 K}{2\pi}}, \\ \langle e^{i\beta\theta(x)} e^{-i\beta\theta(y)}\rangle &\sim |x-y|^{-\frac{\beta^2}{2\pi K}}, \end{aligned} \tag{a19}$$

based on which the scaling dimensions of the vertex operators can be calculated.

By taking $\cos\beta\phi = \frac{1}{2}(e^{i\beta\phi} + e^{-i\beta\phi})$, then

$$\begin{aligned}\langle\cos\beta\phi(x)\cos\beta\phi(y)\rangle &= \frac{1}{4}\Big(\langle e^{i\beta\phi(x)}e^{i\beta\phi(y)}\rangle + \langle e^{i\beta\phi(x)}e^{-i\beta\phi(y)}\rangle \\ &\quad + \langle e^{-i\beta\phi(x)}e^{i\beta\phi(y)}\rangle + \langle e^{-i\beta\phi(x)}e^{-i\beta\phi(y)}\rangle\Big) \\ &\sim |x-y|^{-\frac{\beta^2 K}{2\pi}},\end{aligned}$$

where we have used the fact that $\langle e^{i\beta_1\phi(x_1)}...e^{i\beta_N\phi(x_N)}\rangle = 0$ in the thermodynamic limit when $\sum_{n=1}^{N}\beta_n \neq 0$ [70]. From this we conclude that the scaling dimension of the $\cos\beta\phi$ term is $\frac{\beta^2 K}{4\pi}$. Similarly the $\cos\beta\theta$ term has scaling dimension $\frac{\beta^2}{4\pi K}$. Using these results, the composite operators consisting of this two types of basic vertex operators, like the ones in the main text, can be readily calculated.

A2.2 The one-loop correction

For the one-loop corrections for the RG equations, we consider first the simple case where the free bosonic Lagrangian $\mathcal{L}_0 = \frac{1}{2K}(\partial_\mu\phi)^2$ is perturbed by a generic vortex term $\mathcal{L}' = \frac{g_\phi}{l^{D-\Delta_\phi}}\cos\beta\phi + \frac{g_\theta}{l^{D-\Delta_\theta}}\cos\alpha\theta$, where the short-distance cutoff l is restored to make the couplings dimensionless or scale invariant [60]. The partition function can then be expanded as the following:

$$\begin{aligned}Z &= \int D[\phi]e^{-S} \\ &= Z^*\Big(1 + \int dx\frac{g_\phi}{l^{D-\Delta_\phi}}\langle\cos\beta\phi\rangle + \int dx\frac{g_\theta}{l^{D-\Delta_\theta}}\langle\cos\alpha\theta\rangle \\ &\quad + \frac{1}{2}\int dxdy\frac{g_\phi g_\theta}{l^{2D-\Delta_\phi-\Delta_\theta}}\langle\cos\beta\phi(x)\cos\alpha\theta(y)\rangle \\ &\quad + \frac{1}{2}\int dxdy\frac{g_\phi^2}{l^{2D-2\Delta_\phi}}\langle\cos\beta\phi(x)\cos\beta\phi(y)\rangle \\ &\quad + \frac{1}{2}\int dxdy\frac{g_\theta^2}{l^{2D-2\Delta_\theta}}\langle\cos\alpha\theta(x)\cos\alpha\theta(y)\rangle + O(g^3)\Big), \quad \text{(a20)}\end{aligned}$$

where Z^* represents the free theory partition function. As we know, the conformal invariance of the free theory requires that the cross term corresponding to $g_\phi g_\theta$ vanishes at the one-loop level because the g_ϕ and the g_θ terms in general have different scaling dimensions. So we only need to consider the g_ϕ^2 and g_θ^2 terms.

Firstly, consider the g_ϕ^2 term. The OPE in terms of $e^{i\beta\phi}$ is given by ref. [60],

$$:e^{i\beta\phi(x)}::e^{-i\beta\phi(y)}:= \frac{1}{|x-y|^{2\Delta_\phi}} - \frac{1}{|x-y|^{2\Delta_\phi-2}}\frac{\beta^2}{2}:(\partial_\mu\phi)^2:, \quad \text{(a21)}$$

$$:e^{\pm i\beta\phi(x)}::e^{\pm i\beta\phi(y)}:= \frac{1}{|x-y|^{-2\Delta_\phi}}:e^{\pm i2\beta\phi(x)}:, \quad \text{(a22)}$$

$$:e^{i\alpha\theta(x)}::e^{-i\alpha\theta(y)}:= \frac{1}{|x-y|^{2\Delta_\theta}} - \frac{1}{|x-y|^{2\Delta_\theta-2}}\frac{\alpha^2}{2}:(\partial_\mu\theta)^2:, \quad \text{(a23)}$$

$$:e^{\pm i\alpha\theta(x)}::e^{\pm i\alpha\theta(y)}:= \frac{1}{|x-y|^{2\Delta_\theta}}:e^{\pm i2\alpha\theta(x)}:, \quad \text{(a24)}$$

where it is understood that $|x-y| \to 0$. Therefore,

$$\begin{aligned}&:\cos\beta\phi(x)::\cos\beta\phi(y): \\ &= \frac{1}{4}:\left(e^{i\beta\phi(x)} + e^{-i\beta\phi(x)}\right)::\left(e^{i\beta\phi(y)} + e^{-i\beta\phi(y)}\right): \\ &= \frac{1/2}{|x-y|^{2\Delta_\phi}} - \frac{1/2}{|x-y|^{2\Delta_\phi-2}}\frac{\beta^2}{2}:(\partial_\mu\phi)^2: \\ &\quad + \frac{1/2}{|x-y|^{-2\Delta_\phi}}:\cos 2\beta\phi(x):, \quad \text{(a25)}\end{aligned}$$

and similarly,

$$\begin{aligned}&:\cos\alpha\theta(x)::\cos\alpha\theta(y): \\ &= \frac{1/2}{|x-y|^{2\Delta_\theta}} - \frac{1/2}{|x-y|^{2\Delta_\theta-2}}\frac{\alpha^2}{2}:(\partial_\mu\theta)^2: \\ &\quad + \frac{1/2}{|x-y|^{-2\Delta_\theta}}:\cos 2\alpha\theta(x):. \quad \text{(a26)}\end{aligned}$$

For the g_ϕ^2 term in eq. (a20), $\frac{1}{2}\int dxdy\frac{g_\phi^2}{l^{2D-2\Delta_\phi}}\langle\cos\beta\phi(x)\cos\beta\phi(y)\rangle$, which gives rise to the one-loop correction to the $:(\partial_\mu\phi)^2:$ term, becomes

$$\begin{aligned}&-\frac{\beta^2}{8}\int dxdy\frac{g_\phi^2}{l^{2D-2\Delta_\phi}}|x-y|^{-2\Delta_\phi+2}\langle:(\partial_\mu\phi)^2:\rangle \\ &= -\frac{\beta^2}{8}\int dx\frac{g_\phi^2}{l^{2D-2\Delta_\phi}}\langle:(\partial_\mu\phi)^2:\rangle\int dy|x-y|^{-2\Delta_\phi+2}. \quad \text{(a27)}\end{aligned}$$

Now we do a change of scale by changing the cutoff $l \to l + \delta l = (1 + \delta\ln l)l$. This means the domain of the above integration is changed from $|x-y| > l$ to $|x-y| > (1+\delta\ln l)l$. Therefore, the corresponding change in the above integration becomes

$$\frac{\beta^2}{8}\int dx\frac{g_\phi^2}{l^{2D-2\Delta_\phi}}\langle:(\partial_\mu\phi)^2:\rangle\int_{l<|x-y|<(1+\delta\ln l)l} dy|x-y|^{-2\Delta_\phi+2}, \quad \text{(a28)}$$

which in the case of $D = 2$ is

$$\frac{\beta^2\pi}{4}g_\phi^2\delta\ln l\int dx\langle:(\partial_\mu\phi)^2:\rangle. \quad \text{(a29)}$$

Comparing with the kinetic term $\frac{1}{2K}\int dx(\partial_\mu\phi)^2$, we obtain the correction of K due to the g_ϕ term,

$$\frac{d(1/K)}{d\ln l} = \frac{\pi\beta^2}{2}g_\phi^2 \Rightarrow \frac{dK}{d\ln l} = -\frac{\pi\beta^2K^2}{2}g_\phi^2. \quad \text{(a30)}$$

The contribution from the $g_\theta\cos\alpha\theta$ term can be similarly obtained as:

$$\frac{dK}{d\ln l} = \frac{\pi\alpha^2}{2}g_\theta^2. \quad \text{(a31)}$$

A2.3 Derivation of the RG equations

Using the basic ingredients above, we can proceed to work out the full RG equations presented in the main text. For the free theory given by

$$\mathcal{L}_0 = \frac{1}{4K_+}(\partial_\mu\phi_+)^2+\frac{1}{K_-}(\partial_\mu\phi_-)^2 \equiv \frac{1}{2\tilde{K}_+}(\partial_\mu\phi_+)^2+\frac{1}{2\tilde{K}_-}(\partial_\mu\phi_-)^2, \tag{a32}$$

where we have redefined the Luttinger parameters $\tilde{K}_+ \equiv 2K_+, \tilde{K}_- \equiv K_-/2$, so that the Lagrangian takes the standard normalization convention and the results derived from the previous section can be directly carried over. We have the following scaling dimensions for the different interaction terms:

- For $\cos\beta\phi_+$: $\Delta_{\phi_+} = \frac{\beta^2\tilde{K}_+}{4\pi}$;
- For $\cos\beta\phi_-$: $\Delta_{\phi_-} = \frac{\beta^2\tilde{K}_-}{4\pi}$;
- For $\cos\alpha\theta_-$: $\Delta_{\theta_-} = \frac{\alpha^2}{4\pi\tilde{K}_-}$;
- For $\cos\beta\phi_+\cos\alpha\phi_-$: $\Delta_{\phi_+\phi_-} = \frac{1}{4\pi}\left(\beta^2\tilde{K}_+ + \alpha^2\tilde{K}_-\right)$.

The scaling dimensions above give us the tree-level flow equations. For the loop-level correction of the Luttinger parameters, we again make use of the OPEs. The OPE

$$\begin{aligned}&:\cos\beta\phi_+(x)::\cos\beta\phi_+(y):\\&=\frac{1/2}{|x-y|^{2\Delta_{\phi_+}}}-\frac{1/2}{|x-y|^{2\Delta_{\phi_+}-2}}\frac{\beta^2}{2}:(\partial_\mu\phi_+)^2:,\end{aligned} \tag{a33}$$

gives the following correction after repeating the real-space renormalization,

$$\delta\left(\frac{1}{2\tilde{K}_+}\right) = \frac{1}{2}\cdot\frac{\beta^2}{4}g^2_{\phi_+}\cdot 2\pi\delta(\ln l) \Rightarrow \delta\tilde{K}_+ = -\frac{\pi}{2}\beta^2\tilde{K}_+^2 g^2_{\phi_+}\delta(\ln l). \tag{a34}$$

The OPE

$$\begin{aligned}&:\cos\beta\phi_-(x)::\cos\beta\phi_-(y):\\&=\frac{1/2}{|x-y|^{2\Delta_{\phi_-}}}-\frac{1/2}{|x-y|^{2\Delta_{\phi_-}-2}}\frac{\beta^2}{2}:(\partial_\mu\phi_-)^2:,\end{aligned} \tag{a35}$$

gives the following correction to $\tilde{K}_-$,

$$\delta\left(\frac{1}{2\tilde{K}_-}\right) = \frac{1}{2}\cdot\frac{\beta^2}{4}g^2_{\phi_-}\cdot 2\pi\delta(\ln l) \Rightarrow \delta\tilde{K}_- = -\frac{\pi}{2}\beta^2\tilde{K}_-^2 g^2_{\phi_-}\delta(\ln l). \tag{a36}$$

The OPE

$$\begin{aligned}&:\cos\alpha\theta_-(x)::\cos\alpha\theta_-(y):\\&=\frac{1/2}{|x-y|^{2\Delta_{\theta_-}}}-\frac{1/2}{|x-y|^{2\Delta_{\theta_-}-2}}\frac{\alpha^2}{2}:(\partial_\mu\theta_-)^2:,\end{aligned} \tag{a37}$$

gives the following correction to K_-,

$$\delta\left(\frac{\tilde{K}_-}{2}\right) = \frac{1}{2}\cdot\frac{\alpha^2}{4}g^2_{\theta_-}\cdot 2\pi\delta(\ln l) \Rightarrow \delta\tilde{K}_- = \frac{\pi\alpha^2}{2}g^2_{\theta_-}\delta(\ln l). \tag{a38}$$

The OPE

$$\begin{aligned}&:\cos\beta\phi_+(x)\cos\alpha\phi_-(x)::\cos\beta\phi_+(y)\cos\alpha\phi_-(y):\\&=\frac{1}{16}\sum_{\eta_{1,2,3,4}=\pm1}:\mathrm{e}^{\mathrm{i}(\eta_1\beta\phi_+(x)+\eta_2\alpha\phi_-(x))}::\mathrm{e}^{\mathrm{i}(\eta_3\beta\phi_+(y)+\eta_4\alpha\phi_-(y))}:\\&\Longrightarrow -\frac{1/8}{|x-y|^{2\Delta_{\phi_+}+2\Delta_{\phi_-}-2}}\left(\beta^2:(\partial_\mu\phi_+)^2:+\alpha^2:(\partial_\mu\phi_+)^2:\right)\\&\quad+\frac{1/4}{|x-y|^{-2\Delta_{\phi_+}+2\Delta_{\phi_-}}}:\cos 2\beta\phi_+:\\&\quad+\frac{1/4}{|x-y|^{2\Delta_{\phi_+}-2\Delta_{\phi_-}}}:\cos 2\alpha\phi_-:,\end{aligned} \tag{a39}$$

which generates the following renormalizations:

$$\begin{aligned}\delta\left(\frac{1}{2\tilde{K}_+}\right) &= \frac{1}{2}\cdot\frac{\beta^2}{8}g^2_{\phi_{\rm int}}\cdot 2\pi\delta(\ln l) \Rightarrow \delta\tilde{K}_+\\&= -\frac{\pi\beta^2\tilde{K}_+^2}{4}g^2_{\phi_{\rm int}}\delta(\ln l),\\\delta\left(\frac{1}{2\tilde{K}_-}\right) &= \frac{1}{2}\cdot\frac{\alpha^2}{8}g^2_{\phi_{\rm int}}\cdot 2\pi\delta(\ln l) \Rightarrow \delta\tilde{K}_-\\&= -\frac{\pi\alpha^2\tilde{K}_-^2}{4}g^2_{\phi_{\rm int}}\delta(\ln l),\\\delta g_{\phi_\pm} &= \frac{1}{2}\cdot\frac{1}{4}g^2_{\phi_{\rm int}}\cdot 2\pi\delta(\ln l) = \frac{\pi}{4}g^2_{\phi_{\rm int}}\delta(\ln l).\end{aligned} \tag{a40}$$

Combining the contributions from the different interaction terms, we eventually arrive at the RG equations presented in the main text.

A3 K-matrix formulation of Luttinger liquid

In this section, we review the K-matrix formulation of the Luttinger liquid. In this framework, a Luttinger liquid is treated as the boundary of a higher-dimensional bulk and the K-matrix contains topological information about the bulk. In particular, using the K-matrix it is straightforward to calculate the braiding statistics between the various vertex operators that represent the charges, vortices or their combinations. This is a useful way to rule out non-local operators when writing down the Lagrangian based on symmetry considerations.

A3.1 One pair of boson and dual boson

To warm up for the case of two coupled Luttinger liquids in our paper, we look at the simpler case of one Luttinger liquid

consisting of the boson field θ and its dual ϕ. By defining $\Phi \equiv (\theta, \phi)^{\mathrm{T}}$, the free Lagrangian density is given by

$$\mathcal{L}_0 = \frac{1}{4\pi}\left(\partial_t \Phi^{\mathrm{T}} \mathrm{K} \partial_x \Phi + \partial_x \Phi^{\mathrm{T}} \mathrm{V} \partial_x \Phi\right), \tag{a41}$$

where K is not to be confused with the Luttinger parameter K that appears in the rest part of the paper. The K-matrix is given by $\mathrm{K} = \sigma^1$ and the V-matrix is given by $\mathrm{V} = \sigma^0$, where the σ^μ with $\mu = 0, 1, 2, 3$ are the Pauli matrices. In canonical quantization, the conjugate momentum of the θ field is given by

$$\Pi = \frac{\delta \mathcal{L}_0}{\delta \partial_t \theta} = \frac{1}{2\pi}\partial_x \phi, \tag{a42}$$

with the canonical commutation given by $[\theta(t, x), \Pi(t, y)] = \mathrm{i}\delta(x - y)$, or equivalently, $[\theta(t, x), \partial_y \phi(t, y)] = 2\pi \mathrm{i}\delta(x - y)$.

We have two basic types of vertex operators $\mathrm{e}^{\mathrm{i}\theta}$ and $\mathrm{e}^{\mathrm{i}\phi}$, whose charge vectors are given by $l_\theta = (1, 0)^{\mathrm{T}}$ and $l_\phi = (0, 1)^{\mathrm{T}}$ respectively. Then the braiding statistics between the two vertex operators is given by

$$2\pi l_\theta^{\mathrm{T}} \mathrm{K}^{-1} l_\phi = 2\pi, \tag{a43}$$

which simply states the fact that if we move a charge around its vortex, then it picks up a phase of 2π. Here we take $\mathrm{e}^{\mathrm{i}\theta}$ to be the charge operator and the $\mathrm{e}^{\mathrm{i}\phi}$ to be the vortex operator to be consistent with the notation of the main text. Notice however, that in the normalization convention of the main text, the vortex is given by $\mathrm{e}^{\mathrm{i}2\pi\phi}$ instead, so there is a factor of 2π in the field rescaling for ϕ. In the convention used here, θ and ϕ are put on equal footing, both without the π factors. The normalization convention does not change the essential physics we discuss.

A3.2 Two coupled Luttinger liquids

Now we move on to two coupled Luttinger liquids, which would correspond to two coupled XY-models. Choosing the basis $\Phi = (\theta_1, \phi_1, \theta_2, \phi_2)^{\mathrm{T}}$, the Lagrangian density takes the same form as in eq. (a41), but the new K-matrix and V-matrix are given by

$$\mathrm{K} = \begin{pmatrix} \sigma^x & 0 \\ 0 & \sigma^x \end{pmatrix}, \quad \mathrm{V} = \begin{pmatrix} \sigma^0 & 0 \\ 0 & \sigma^0 \end{pmatrix}. \tag{a44}$$

Then we have the following charge vectors:

$$\begin{aligned} l_{\theta_1} &= (1, 0, 0, 0)^{\mathrm{T}}, \quad l_{\phi_1} = (0, 1, 0, 0)^{\mathrm{T}}, \\ l_{\theta_2} &= (0, 0, 1, 0)^{\mathrm{T}}, \quad l_{\phi_2} = (0, 0, 0, 1)^{\mathrm{T}}. \end{aligned} \tag{a45}$$

Under the basis transformation used in the main text,

$$\begin{aligned} &\theta_+ \equiv (\theta_1 + \theta_2)/2, \ \theta_- \equiv \theta_1 - \theta_2, \\ &\phi_+ \equiv \phi_1 + \phi_2, \qquad \phi_- \equiv (\phi_1 - \phi_2)/2, \end{aligned} \tag{a46}$$

the charge vectors for the new fields are given by

$$\begin{aligned} l_{\theta_+} &= \left(\frac{1}{2}, 0, \frac{1}{2}, 0\right)^{\mathrm{T}}, \quad l_{\phi_+} = (0, 1, 0, 1)^{\mathrm{T}}, \\ l_{\theta_-} &= (1, 0, -1, 0)^{\mathrm{T}}, \quad l_{\phi_-} = \left(0, \frac{1}{2}, 0, -\frac{1}{2}\right)^{\mathrm{T}}. \end{aligned} \tag{a47}$$

In a similar fashion, the braidings between the fields and the dual fields are given by

$$\begin{aligned} &2\pi l_{\theta_+}^{\mathrm{T}} \mathrm{K}^{-1} l_{\phi_+} = 2\pi, \quad 2\pi l_{\theta_-}^{\mathrm{T}} \mathrm{K}^{-1} l_{\phi_-} = 2\pi, \\ &2\pi l_{\theta_+}^{\mathrm{T}} \mathrm{K}^{-1} l_{\phi_-} = 0, \quad 2\pi l_{\theta_-}^{\mathrm{T}} \mathrm{K}^{-1} l_{\phi_+} = 0, \end{aligned} \tag{a48}$$

i.e., the braidings between fields from different channels vanish, as it should be.

Now we are ready to check the locality of the various terms appearing in the Lagrangian, i.e., whether their braiding with the original local physical fields $\theta_{1,2}$ are integer multiples of 2π.

- $\cos\phi_+$ (note again that this term is the $\cos 2\pi\phi_+$ in the main text): The charge vector is $(0, 1, 0, 1)^{\mathrm{T}}$, and its braiding with $\theta_{1,2}$ are both 2π. Higher order terms are therefore also allowed.
- $\cos 2\theta_-$: The charge vector is $(1, 0, 1, 0)^{\mathrm{T}}$, and its braiding with $\theta_{1,2}$ are both 0.
- $\cos\phi_-$ (equivalent to $\cos 2\pi\phi_-$ in the main text): The charge vector is $(0, \frac{1}{2}, 0, -\frac{1}{2})^{\mathrm{T}}$, and its braiding with $\theta_{1,2}$ are $\pm\pi$ respectively, i.e., not integer multiple of 2π, hence not allowed.
- $\cos 2\phi_-$ (equivalent to $\cos 4\pi\phi_-$ in the main text): The charge vector is $(0, 1, 0, -1)^{\mathrm{T}}$, and its braiding with $\theta_{1,2}$ are $\pm 2\pi$.
- $\cos\frac{1}{2}\phi_+ \cos\phi_-$ (equivalent to $\cos\pi\phi_+ \cos 2\pi\phi_-$ in the main text): The charge vector is given by $(0, 1, 0, 0)^{\mathrm{T}}$, whose braiding with $\theta_{1,2}$ are 2π and 0 respectively, hence it is local and allowed, even though neither $\cos\frac{1}{2}\phi_+$ nor $\cos\phi_-$ is allowed separately. This is consistent with the fact that this term comes from the sum of the original two local vortex terms $\cos\phi_1$ and $\cos\phi_2$.